

14. Bjerregaard, P., Gussak, I., Kotar, S. L., Gessler, J. E. & Janosik, D. Recurrent syncope in a patient with prominent J wave. *Am. Heart J.* **127**, 1426–1430 (1994).
15. Miyazaki, T. *et al.* Autonomic and antiarrhythmic drug modulation of ST segment elevation in patients with Brugada syndrome. *J. Am. Coll. Cardiol.* **27**, 1061–1070 (1996).
16. Tung, R. T., Shen, W., Hammil, S. C. & Gersh, E. J. Idiopathic ventricular fibrillation in out-of-hospital cardiac arrest survivors. *PACE* **17**, 1405–1411 (1994).
17. Cobb, L. A. in *Hurst's The Heart* (eds Schlant, R. C. & Alexander, R. W.) 8th edn. 947–957 (McGraw Hill, New York, 1994).
18. Wang, Q., Li, Z., Shen, J. & Keating, M. T. Genomic organization of the human *SCN5A* gene encoding the cardiac sodium channel. *Genomics* **34**, 9–16 (1996).
19. Rogers, J. C., Qu, Y., Tanada, T. N., Scheuer, T. & Catterall, W. A. Molecular determinants of high affinity binding of α -scorpion toxin and sea anemone toxin in the S3–S4 extracellular loop in domain IV of the Na channel α subunit. *J. Biol. Chem.* **271**, 15950–15962 (1996).
20. Hoffman, E. P., Lehmann-Horn, F. & Rudel, R. Overexcited or inactive: ion channels in muscle disease. *Cell* **80**, 681–686 (1995).
21. Yang, N. & Horn, R. Evidence for voltage-dependent S4 movement in sodium channels. *Neuron* **15**, 213–218 (1995).
22. Shapiro, M. B. & Senapathy, P. RNA splice junctions of different classes of eukaryotes: sequence statistics and functional implications in gene expression. *Nucleic Acids Res.* **15**, 7155–7174 (1987).
23. Wang, Q. *et al.* *SCN5A* mutations associated with an inherited cardiac arrhythmia, long QT syndrome. *Cell* **80**, 805–811 (1995).
24. Wang, Q. *et al.* Cardiac sodium channel mutations in patients with long QT syndrome, an inherited cardiac arrhythmia. *Hum. Mol. Genetics* **4**, 1603–1607 (1995).
25. Bennett, P. B., Yazawa, K., Makita, N. & George, A. L. Jr Molecular mechanism for an inherited cardiac arrhythmia. *Nature* **376**, 683–685 (1995).
26. Dumaine, R. *et al.* Multiple mechanisms of Na⁺ channel-linked long-QT syndrome. *Circulation Res.* **78**, 916–922 (1996).
27. Stuhmer, W. *et al.* Structural parts involved in activation and inactivation of the sodium channel. *Nature* **339**, 597–603 (1989).
28. Krishnan, S. C. & Antzelevitch, C. Sodium channel block produces opposite electrophysiological effects in canine ventricular epicardium and endocardium. *Circulation Res.* **69**, 277–291 (1991).
29. Krishnan, S. C. & Antzelevitch, C. Flecainide-induced arrhythmia in canine ventricular epicardium. Phase 2 reentry? *Circulation* **87**, 562–572 (1992).
30. Yan, G. X. & Antzelevitch, C. Cellular basis for the electrocardiographic J wave. *Circulation* **93**, 372–379 (1996).

Acknowledgements. We thank H. Hartmann for the wild-type *SCN5A* construct; M. Sanguinetti and P. Spector for help with electrophysiological analysis of the 1-bp deletion; and P. Szafranski, J. T. Bricker, M. Scheinman, A. L. Beudet, A. Bradley and X. Qu for help and advice. This work was supported by a Grant-In-Aid from the American Heart Association, by the AHA, Northeast Ohio Affiliate (G.E.K.), and the Deutsche Forschungsgemeinschaft (E.S.-B.), and by grants from the NIH and Bristol-Myers Squibb (M.T.K.), The Texas Children's Hospital Foundation Chair in Pediatric Cardiac Research and NIH grants (J.A.T.), the Carolien Weiss Law Grant for Research in Molecular Medicine (Q.W.), the Abercrombie Cardiology Fund of Texas Children's Hospital (Q.W.), and a Scientist Development Award from the American Heart Association (Q.W.).

Correspondence and requests for materials should be addressed to Q.W. (e-mail: qwang@bcm.tmc.edu).

Fas-mediated apoptosis and activation-induced T-cell proliferation are defective in mice lacking FADD/Mort1

Jianke Zhang, Dragana Cado, Ann Chen, Nisha H. Kabra & Astar Winoto

Department of Molecular and Cell Biology, Division of Immunology and Cancer Research Laboratory, University of California at Berkeley, 469 LSA, Berkeley, California 94720-3200, USA

Programmed cell death, or apoptosis, is important in homeostasis of the immune system: for example, non-functional or auto-reactive lymphocytes are eliminated through apoptosis. One member of the tumour necrosis factor receptor (TNFR) family, Fas (also known as CD95 or Apo-1), can trigger cell death and is essential for lymphocyte homeostasis^{1,2}. FADD/Mort1 (refs 3–6) is a Fas-associated protein that is thought to mediate apoptosis by recruiting the protease caspase-8 (refs 7, 8). A dominant-negative mutant of FADD inhibits apoptosis initiated by Fas and other TNFR family members^{6,9–14}. Other proteins, notably Daxx, also bind Fas and presumably mediate a FADD-independent apoptotic pathway¹⁵. Here we investigate the role of FADD *in vivo* by generating FADD-deficient mice. As homozygous mice die *in utero*, we generated *FADD*^{-/-} embryonic stem cells and *FADD*^{-/-} chimaeras in a background devoid of the recombination activating gene *RAG-1*, which activates rearrangement of the immunoglobulin and T-cell receptor genes. We found that thymocyte subpopulations were apparently normal in newborn chimaeras.

Fas-induced apoptosis was completely blocked, indicating that there are no redundant Fas apoptotic pathways. As these mice age, their thymocytes decrease to an undetectable level, although peripheral T cells are present in all older *FADD*^{-/-} chimaeras. Unexpectedly, activation-induced proliferation is impaired in these *FADD*^{-/-} T cells, despite production of the cytokine interleukin (IL)-2. These results and the similarities between *FADD*^{-/-} mice and mice lacking the β -subunit of the IL-2 receptor suggest that there is an unexpected connection between cell proliferation and apoptosis.

To generate FADD-deficient mice we replaced the first exon of FADD with a neomycin-resistance (neo) gene (Fig. 1a). Heterozygous mutant embryonic stem (ES) cells were identified by Southern blot analysis (Fig. 1b), and *FADD*^{+/-} mice were produced from three *FADD*^{+/-} ES lines. Interbreeding of these mice, however, yielded only heterozygous and wild-type mice in a 2:1 ratio. Subsequent studies established that *FADD*^{-/-} embryos die at around day 9 of gestation (data not shown), indicating that FADD is essential for embryonic development.

Because Fas is necessary for homeostasis in the immune system, we sought to investigate the effect of FADD deletion in lymphoid organs. However, this can not be examined directly because *FADD*^{-/-} mice die *in utero*. We therefore made *FADD*^{-/-} ES cells and injected them into C57BL/6-*RAG-1*^{-/-} (B6-*RAG-1*^{-/-}) blastocysts to generate *FADD*^{-/-} chimaeras¹⁶. Homozygous *FADD*^{-/-} ES cells were obtained by subjecting *FADD*^{+/-} ES cells to a high level of G418 selection¹⁷ (Fig. 1b). Complete absence of FADD protein was confirmed by western blot analysis (Fig. 1c). Because these ES donor cells originate from 129/Sv strain (agouti colour) and host blastocysts originate from B6-*RAG-1*^{-/-} mice (black), chimaeras were readily identified by coat colour. By this means we generated 20 viable chimaeras. All mature lymphocytes in these *FADD*^{-/-} → *RAG-1*^{-/-} chimaeras (designated *FADD*^{-/-}) are derived from *FADD*^{-/-} ES cells because *RAG-1*^{-/-} mice are not capable of producing any B or T cells¹⁸. An antibody for the allelic Ly9.1 antigen provides another means of distinguishing the donor (129/Sv mice are Ly9.1⁺) from the host cells (B6 mice are Ly9.1⁻). Tissue Southern blot analysis confirmed the contribution of *FADD*^{-/-} ES cells in many organs and tissues (data not shown).

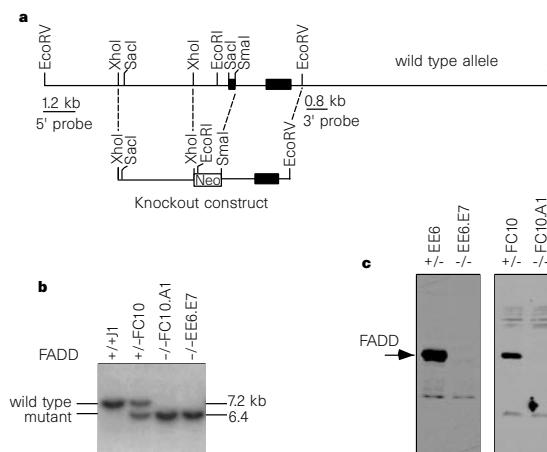


Figure 1 Targeted inactivation of the gene encoding FADD/Mort1 in ES cells and in mice. **a**, A restriction map of the murine *FADD* locus is shown (filled boxes denote exons)⁶. A schematic representation of the FADD targeting construct is shown underneath. **b**, Generation of FADD-deficient ES cell clones. Heterozygous ES cell clones were identified by Southern blots with 5' probe which detects a 7.2-kilobase (*EcoRI*-*EcoRV*) wild-type allele and a 6.4-kb mutant allele. Two *FADD*^{-/-} clones, FC10.A1 and EE6.E7, were obtained after further G418 selection¹⁷. They contain only the mutant alleles. J1 is the parental wild-type ES cell for FC10. **c**, The absence of FADD protein in *FADD*^{-/-} lines was confirmed by western blot analysis using anti-FADD antibodies⁶.

We analysed the cellular profile of thymi from *FADD*^{-/-} chimaeras. Thymic cellularity of newborn to 5-week-old *FADD*^{-/-} chimaeras ($10.8 \pm 2.3 \times 10^6$, $n = 7$) is not significantly greater than that of *RAG-1*^{-/-} mice ($9.3 \pm 2.9 \times 10^6$, $n = 5$). However, *RAG-1*^{-/-} chimaeras reconstituted with the wild-type ES cells have a similar number of thymic cells to wild-type mice. Thus *FADD*^{-/-} donor ES cells seem to be inefficient in reconstituting and/or maintaining thymic cellularity. T-cell development in *RAG-1*^{-/-} mice is blocked at the CD4⁺CD8⁻ stage¹⁸ (Fig. 2). In contrast, newborn and 4-day-old *FADD*^{-/-} chimaeras have thymocyte subsets resembling those of wild-type mice (Fig. 2). All CD4⁺CD8⁺ double-positive and single-positive cells are Ly9.1⁺, confirming their ES cell origin. As the chimaeras age, however, the population of *FADD*^{-/-} thymocytes greatly diminishes. By five weeks, few or no double-positive thymocytes remain (Fig. 2). Nevertheless, the mature Ly9.1⁺ T lymphocytes (CD3⁺) are present in peripheral organs (Fig. 3).

It is possible that the disappearance of thymocytes over time could result from an intrinsic survival defect of *FADD*^{-/-} cells. Alternatively, *FADD*^{-/-} cells might cause some physiological changes in the thymus, such as production of cytotoxic cytokines. This latter possibility is unlikely because chimaeras in wild-type background (*FADD*^{-/-} → B6) have a normal number of host Ly9.1⁻ thymocytes. *FADD*^{-/-} thymocytes seem to die faster *in vitro* than their wild-type counterparts (data not shown), suggesting that *FADD*^{-/-} thymocytes have an intrinsic defect.

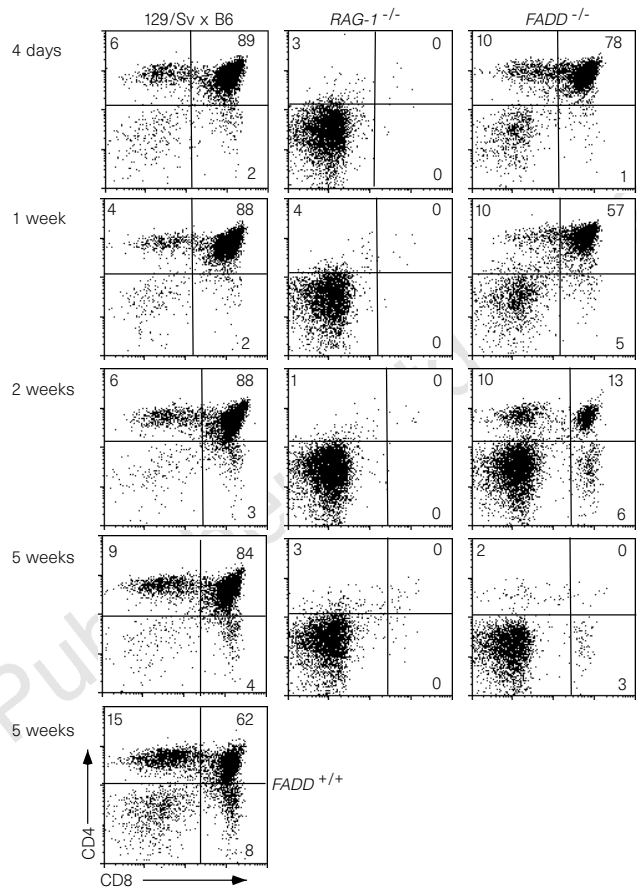


Figure 2 Flow cytometric analysis of thymocytes from wild-type 129/Sv × B6, *RAG-1*^{-/-}, *FADD*^{-/-} to *RAG-1*^{-/-} (*FADD*^{-/-}), and *FADD*^{+/+} to *RAG-1*^{-/-} (*FADD*^{+/+}) mice. Thymocytes from mice with ages indicated were analysed with anti-CD4 and anti-CD8 antibodies. The percentage of each population is indicated in each quadrant.

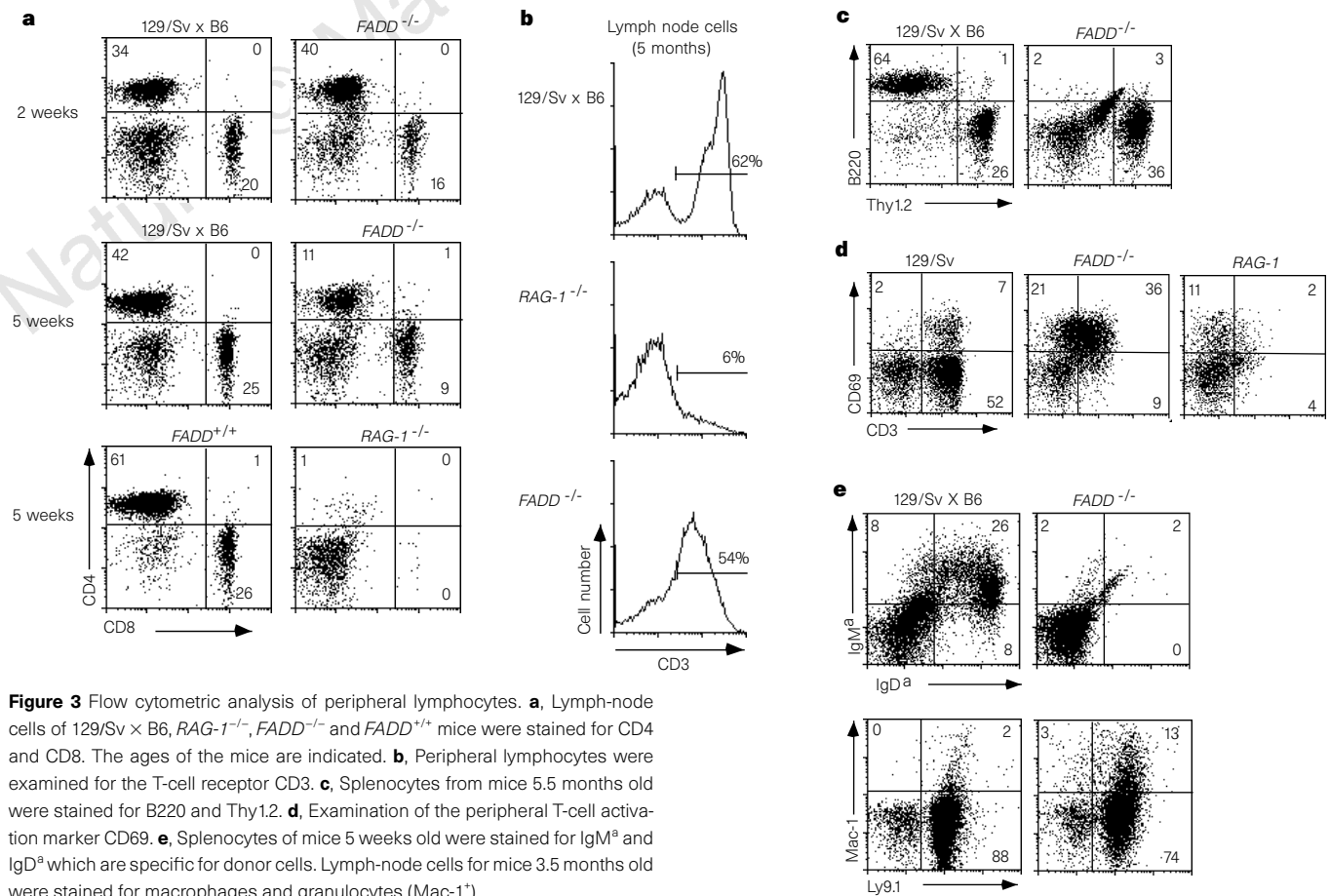
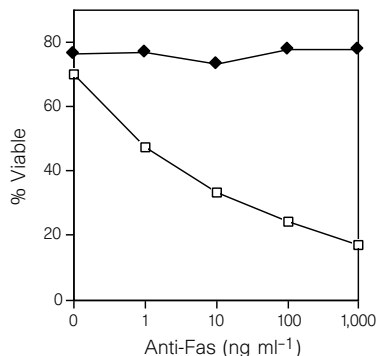


Figure 3 Flow cytometric analysis of peripheral lymphocytes. **a**, Lymph-node cells of 129/Sv × B6, *RAG-1*^{-/-}, *FADD*^{-/-} and *FADD*^{+/+} mice were stained for CD4 and CD8. The ages of the mice are indicated. **b**, Peripheral lymphocytes were examined for the T-cell receptor CD3. **c**, Splenocytes from mice 5.5 months old were stained for B220 and Thy1.2. **d**, Examination of the peripheral T-cell activation marker CD69. **e**, Splenocytes of mice 5 weeks old were stained for IgM^β and IgD^β which are specific for donor cells. Lymph-node cells for mice 3.5 months old were stained for macrophages and granulocytes (Mac-1⁺).

In contrast to the thymus, *FADD*^{-/-} mice contain large numbers of T cells in peripheral lymphoid organs. The total number of *FADD*^{-/-} splenocytes ($23.4 \pm 9.6 \times 10^6$, $n = 8$) is reduced roughly twofold compared with that of the wild-type counterparts ($54.5 \pm 13.1 \times 10^6$, $n = 7$); *RAG-1*^{-/-} mice have fewer splenocytes ($8.73 \pm 3.1 \times 10^6$, $n = 6$). The lymph-node cell number of *FADD*^{-/-} mice is similar to that of wild-type mice (*FADD*^{-/-}, $28.3 \pm 8.6 \times 10^6$, $n = 6$; wild type, $36.4 \pm 3.7 \times 10^6$, $n = 5$; *RAG-1*^{-/-}, $4.7 \pm 3.1 \times 10^6$, $n = 4$). Single-positive (CD3⁺) T cells are present in both *FADD*^{-/-} lymph nodes (Fig. 3a, b) and spleens.



◀ **Figure 4** Fas-mediated cell death is blocked in the absence of FADD. Thymocytes from *FADD*^{+/+} (open squares) and *FADD*^{-/-} (filled diamonds) mice 4 days old were incubated with increasing concentrations of the anti-Fas antibody Jo2 in the presence of cycloheximide as described²². Viability was determined by propidium iodide exclusion. Values are averages of duplicates. The same analysis was performed on mice 1 and 2 weeks old with similar results.

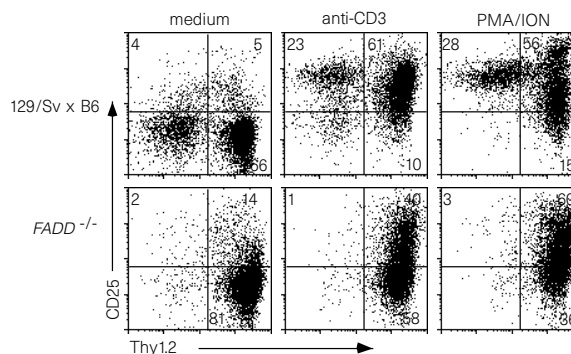
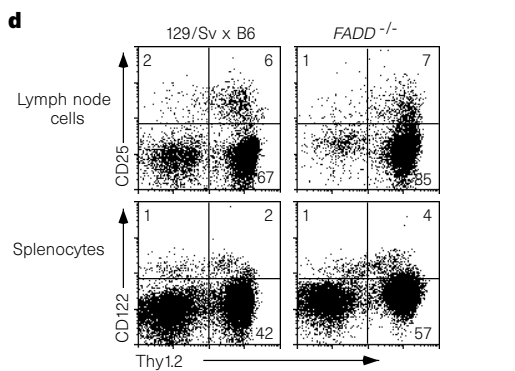
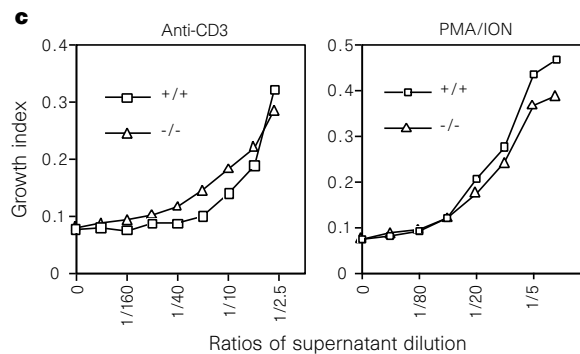
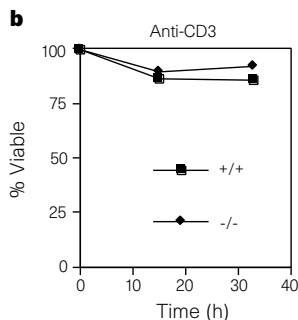
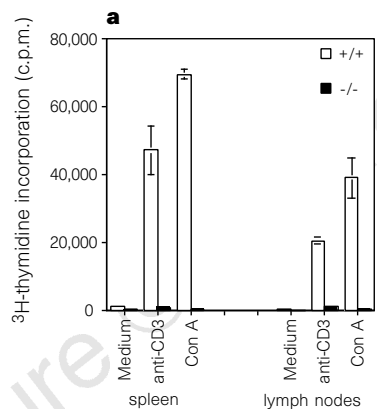


Figure 5 T-cell proliferation and death and IL-2 secretion assay. **a**, Lymphocytes from *FADD*^{+/+} (white bars) and *FADD*^{-/-} (black bars) mice 3.5 months old were treated with anti-CD3 antibody or concanavalin A. Proliferation was monitored by [³H]thymidine incorporation. The experiment was done in triplicate. Similar results were observed with mice two weeks old. **b**, Cell viability of anti-CD3 stimulated lymph-node T cells (Thy1.2⁺) was followed by staining with 7-amino-actinomycin D and flow cytometry as described²⁰. +/+, squares; -/-, diamonds. **c**, IL-2 production from stimulated splenocytes was determined by CTL2 survival and MTT assay. **d**, Unstimulated (top) or stimulated (bottom) lymph-node cells were stained for CD25 and splenocytes for CD122.

IgM^a and IgD^a, which are allele-specific for the 129/Sv strain, to distinguish donor from host cells. Strikingly, *FADD*^{-/-} chimaeras do not contain detectable levels of Ly9.1⁺B220⁺IgM^aIgD^aB cells in either bone marrow or spleen (Fig. 3c, e), which may indicate that deletion of *FADD* leads to a blockage of B-cell development. Using Ly9.1 as a donor cell marker, we examined other haematopoietic cells in *FADD*^{-/-} chimaeras. Macrophages and granulocytes (Ly9.1⁺Mac-1⁺) are present in *FADD*^{-/-} mice (Fig. 3e). The high proportion of Ly9.1⁺Mac-1⁺ cells in these *FADD*^{-/-} mice is probably due to the absence of B lymphocytes.

Proteins other than *FADD* have also been reported to bind to Fas^{15,19–21}. Expression of one of these Fas-interacting proteins, Daxx, potentiates Fas-induced apoptosis in an apparently *FADD*-independent manner, suggesting that there are parallel apoptotic pathways downstream of Fas¹⁵. To investigate this, we incubated *FADD*^{-/-} thymocytes with an agonist anti-Fas antibody²². Both thymic and peripheral T cells in *FADD*^{-/-} chimaeric mice express Fas at a high level, comparable to that of wild-type T cells (data not shown). Wild-type thymocytes are killed in a dose-dependent manner (Fig. 4). In contrast, thymocytes from *FADD*^{-/-} mice are completely resistant to the cytotoxic effect of anti-Fas antibody. Thus *FADD* is an essential mediator of Fas-induced apoptosis and there is unlikely to be a parallel apoptotic pathway downstream of Fas. Although thymocytes are less sensitive to TNF-mediated apoptosis (twofold effect)²³, our results also showed that *FADD*^{-/-} thymocytes are more resistant to this than their wild-type counterparts (data not shown).

The absence in *FADD*^{-/-} mice of lymphoproliferative disease and the T-cell population characteristic of Fas mutant mice may result from a defect in the activation and proliferation of T cells. To examine this possibility, peripheral lymphocytes of age-matched wild-type and *FADD*^{-/-} mice were stimulated with an anti-CD3 antibody or concanavalin A (Con A). Wild-type T cells proliferated extensively, whereas *FADD*^{-/-} peripheral T cells did not (Fig. 5a). The lack of proliferation is not due to the death of *FADD*^{-/-} peripheral T cells during stimulation, as no differences in cell viability were observed between wild-type and mutant cells (Fig. 5b).

To establish whether the reduced proliferation of *FADD*^{-/-} T cells results from the lack of IL-2 production or unresponsiveness to IL-2, we assayed for the secretion of IL-2. After stimulation, *FADD*^{-/-} cells produced wild-type levels of IL-2, as shown by bioassay and enzyme-linked immunosorbent assay (ELISA) (Fig. 5c and data not shown). Freshly isolated mutant T cells have normal levels of IL-2R α (CD25) and IL-2R β (CD122) (Fig. 5d, top). Activation of T cells leads to a dramatic induction of CD25 expression in both wild-type and mutant T cells (Fig. 5d, bottom). Thus *FADD*^{-/-} T cells fail to proliferate despite there being normal levels of IL-2R and IL-2 production.

We have shown that *in vivo* *FADD* is essential for Fas-induced apoptosis and that there is no parallel Fas apoptotic pathway. As mice with mutations in either Fas or TNF-R1 are viable, we were surprised to find that deletion of *FADD* leads to embryonic lethality. Because other apoptotic receptors can interact with *FADD*^{10–14}, their function may be necessary during embryogenesis. Alternatively, *FADD* may be involved in other signalling pathways required for development and proliferation, as *FADD* seems to be required for T-cell proliferation. Although these phenotypes could arise from abnormal T-cell development in the absence of *FADD*, we believe that they reflect direct roles of *FADD in vivo*. Several characteristics of *FADD*-deficient chimaeras are strikingly similar to those of IL-2R β -deficient mice²⁴, including the defect in T-cell proliferation in response to IL-2, a higher percentage of CD69⁺ T cells, and age-dependent disappearance of thymocytes²⁴. These data suggest that *FADD* is involved in cytokine signalling. IL-2 is implicated in T-cell apoptosis^{25–28} as well as being involved in proliferation. Production of IL-2 in response to T-cell receptor stimulation leads to proliferation

as well as sensitization to Fas-mediated apoptosis^{25,26}. Further studies are required to show how *FADD* mediates distinct pathways of death and growth, and the molecular relationship between them. □

Methods

Generation of *FADD*^{-/-} mice and *RAG-1*^{-/-} chimaeras. *FADD*^{+/-} and *FADD*^{-/-} ES cells and mice were generated as described²⁹. Chimaeras were analysed by flow cytometry using monoclonal antibodies (Caltag and Pharmingen).

IL-2 secretion and proliferation assay. Splenocytes or lymph-node cells were stimulated with anti-CD3 ascites (1:3,000 dilution) or PMA (5 ng ml⁻¹) and ionomycin (A23187, 60 ng ml⁻¹) or Con A (5 μ g ml⁻¹). After 14 h incubation at 37 °C, cells were collected, and expression of the α and β subunits of the IL-2 receptor was examined by flow cytometry. To determine IL-2 concentration, the culture supernatants were diluted and assayed by CTLL-2 proliferation bioassay using MTT (3-(4,5-dimethyl-thiazol-2-yl) 2,5-diphenyltetrazolium bromide). For proliferation assay, lymph-node cells or splenocytes were seeded in 96-well culture dishes (2 \times 10⁶ ml⁻¹). Anti-CD3 ascites, PMA plus ionomycin, or Con A was added as described above. After 48 h incubation at 37 °C, [³H]thymidine (1 μ Ci) was then added to each sample. [³H]Thymidine incorporation was quantified 12 h later.

Received 26 November 1997; accepted 5 February 1998.

- Nagata, S. & Golstein, P. The Fas death factor. *Science* **267**, 1449–1455 (1995).
- Matiba, B., Mariani, S. M. & Krammer, P. H. The CD95 system and the death of a lymphocyte. *Semin. Immunol.* **9**, 59–68 (1997).
- Boldin, M. P. et al. A novel protein that interacts with the death domain. *J. Biol. Chem.* **270**, 7795–7798 (1995).
- Chinnaiyan, A. M., O'Rourke, K., Tewari, M. & Dixit, V. M. *FADD*, a novel death domain-containing protein, interacts with the death domain of Fas and initiates apoptosis. *Cell* **81**, 505–512 (1995).
- Kischkel, F. C. et al. Cytotoxicity-dependent APO-1 (Fas/CD95) associated proteins form a death-inducing signaling complex (DISC) with the receptor. *EMBO J.* **14**, 5579–5588 (1995).
- Zhang, J. & Winoto, A. A mouse Fas-associated protein with homology to the human MORT1/*FADD* protein is essential for Fas-induced apoptosis. *Mol. Cell. Biol.* **16**, 2756–2763 (1996).
- Muzio, M. et al. FLICE, a novel *FADD*-homologous ICE/CED-3-like protease, is recruited to the CD95 (Fas/APO-1) death-inducing signaling complex. *Cell* **85**, 817–827 (1996).
- Boldin, M. P., Goncharov, T. M., Goltsev, Y. V. & Wallach, D. Involvement of MACH, a novel MORT1/*FADD*-interacting protease, in Fas/APO-1 and TNF receptor-induced cell death. *Cell* **85**, 803–815 (1996).
- Chinnaiyan, A. M. et al. *FADD*/MORT1 is a common mediator of CD95 (Fas/APO-1) and tumor necrosis factor receptor-induced apoptosis. *J. Biol. Chem.* **271**, 4961–4965 (1996).
- Hsu, H., Shu, H.-B., Pan, M.-G. & Goeddel, D. V. TRADD-TRAF2 and TRADD-*FADD* interactions define two distinct TNF receptor 1 signal transduction pathways. *Cell* **84**, 299–308 (1996).
- Bodmer, J.-L. et al. TRAMP, a novel apoptosis-inducing receptor with sequence homology to tumor necrosis factor receptor 1 and Fas(Apo-1/CD95). *Immunity* **6**, 79–88 (1997).
- Chinnaiyan, A. M. et al. Signal transduction by DR3, a death domain-containing receptor related to TNFR-1 and CD95. *Science* **274**, 990–992 (1996).
- Kitson, J. et al. A death-domain-containing receptor that mediates apoptosis. *Nature* **384**, 372–375 (1996).
- Marsters, S. A. et al. Apo-3, a new member of the tumor necrosis factor receptor family, contains a death domain and activates apoptosis and NF- κ B. *Curr. Biol.* **6**, 1669–1676 (1996).
- Yang, X., Khosravi-Far, R., Chang, H. Y. & Baltimore, D. Daxx, a novel Fas-binding protein that activates JNK and apoptosis. *Cell* **89**, 1067–1076 (1997).
- Chen, J., Lansford, R., Stewart, V., Young, F. & Alt, F. W. *RAG-2*-deficient blastocyst complementation: An assay of gene function in lymphocyte development. *Proc. Natl. Acad. Sci. USA* **90**, 4528–4532 (1993).
- Mortensen, R. M., Conner, D. A., Chao, S., Geisterfer-Lowrance, A. A. & Seidman, J. G. Production of homozygous mutant ES cells with a single targeting construct. *Mol. Cell. Biol.* **12**, 2391–2395 (1992).
- Mombaerts, P. et al. *RAG-1*-deficient mice have no mature B and T lymphocytes. *Cell* **68**, 869–877 (1992).
- Chu, K., Niu, X. & Williams, L. T. A Fas-associated protein factor, FAF1, potentiates Fas-mediated apoptosis. *Proc. Natl. Acad. Sci. USA* **92**, 11894–11898 (1995).
- Sato, T., Irie, S., Kitada, S. & Reed, J. C. FAP-1: a protein tyrosine phosphatase that associates with Fas. *Science* **268**, 411–415 (1995).
- Stanger, B. Z., Leder, P., Lee, T.-H., Kim, E. & Seed, B. RIP: a novel protein containing a death domain that interacts with Fas/APO-1 (D95) in yeast and causes cell death. *Cell* **81**, 513–523 (1995).
- Ogasawara, J., Suda, T. & Nagata, S. Selective apoptosis of CD4⁺CD8⁺ thymocytes by the anti-Fas antibody. *J. Exp. Med.* **181**, 485–491 (1995).
- Hernandez-Caselles, T. & Stutman, O. Immune functions of tumor necrosis factor. *J. Immunology* **151**, 3999–4012 (1993).
- Suzuki, H. et al. Derregulated T cell activation and autoimmunity in mice lacking interleukin-2 receptor β . *Science* **268**, 1472–1476 (1995).
- Fournel, S., Genestier, L., Robinet, E., Flacher, M. & Revillard, J.-P. Human T cells require IL-2 but not G_i/S transition to acquire susceptibility to Fas-mediated apoptosis. *J. Immunol.* **157**, 4309–4315 (1996).
- Lenardo, M. J. The molecular regulation of lymphocyte apoptosis. *Semin. Immunol.* **9**, 1–5 (1997).
- Parisi, L. V. et al. Functional responses and apoptosis of CD25 (IL-2R α)-deficient T cells expressing a transgenic antigen receptor1. *J. Immunol.* **158**, 3738–3745 (1997).
- Lenardo, M. J. Interleukin-2 programs mouse alpha beta T lymphocytes for apoptosis. *Nature* **353**, 858–861 (1991).
- Ramirez-Solis, R., Davis, A. C. & Bradley, A. Gene targeting in embryonic stem cells. *Methods Enzymol.* **225**, 855–878 (1993).
- Schmid, L., Uittenbogaart, C. H., Keld, B. & Giorgi, J. V. A rapid method for measuring apoptosis and dual-color immunofluorescence by single laser flow cytometry. *J. Immunol. Methods* **170**, 145–157 (1994).

Acknowledgements. We thank members of the Winoto, Allison, Robey and Raulet groups for discussions; P. Schow for technical assistance; A. Nagy, R. Nagy and W. Abramow-Newerly for the R1 ES cells; R. Jaenisch for the J1 ES cells; and E. Robey, B. Ortiz and H. Kasler for critical reading of the manuscript. This work is supported in part by grants from the NIH, National Science foundation and the Keck Foundation. J.Z. was supported by an Irvington Institute fellowship and is a Leukemia Society of America special fellow.

Correspondence and requests for materials should be addressed to A.W. (e-mail: winoto@uclink2.berkeley.edu).

Mutations of mitotic checkpoint genes in human cancers

Daniel P. Cahill^{*†}, Christoph Lengauer^{*†}, Jian Yu^{*}, Gregory J. Riggins^{*}, James K. V. Willson[‡], Sanford D. Markowitz[‡], Kenneth W. Kinzler^{* &} Bert Vogelstein^{*}

^{*} The Johns Hopkins Oncology Center, Program in Human Genetics, and The Howard Hughes Medical Institute, Johns Hopkins University School of Medicine, 424 North Bond Street, Baltimore, Maryland 21231, USA

[‡]Department of Medicine and Ireland Cancer Center, Case Western Reserve University and The Howard Hughes Medical Institute, Cleveland, Ohio 44106, USA

[†] These authors contributed equally to this study.

Genetic instability was one of the first characteristics to be postulated to underlie neoplasia¹⁻³. Such genetic instability occurs in two different forms. In a small fraction of colorectal and some other cancers, defective repair of mismatched bases results in an increased mutation rate at the nucleotide level and consequent widespread microsatellite instability⁴⁻⁷. In most colorectal cancers, and probably in many other cancer types, a chromosomal instability (CIN) leading to an abnormal chromosome number (aneuploidy) is observed⁸. The physiological and molecular bases of this pervasive abnormality are unknown. Here we show that CIN is consistently associated with the loss of function of a mitotic checkpoint. Moreover, in some cancers displaying CIN the loss of this checkpoint was associated with the mutational inactivation of a human homologue of the yeast *BUB1* gene; *BUB1* controls mitotic checkpoints and chromosome segregation in yeast. The normal mitotic checkpoints of cells

displaying microsatellite instability become defective upon transfer of mutant *hBUB1* alleles from either of two CIN cancers.

The key insight leading to the discovery of the molecular basis of microsatellite instability (MIN) in human tumours was the discovery of a similar phenotype in *Saccharomyces cerevisiae* cells carrying mutations in yeast mismatch repair (MMR) genes⁹. Following this paradigm, we reasoned that the basis for CIN in human tumour cells might be mitotic checkpoint defects similar to those previously observed in yeast cells with chromosomal instability¹⁰⁻¹². Cells with such defects are expected to exit mitosis prematurely after treatment with microtubule-disrupting agents^{12,13}. To test this hypothesis in human colorectal cancer cells, we treated four MIN lines (HCT116, DLD1, RKO, and SW48) and six CIN lines (SW480, HT29, V400, V429, Caco2, and SW837) with nocodazole, a microtubule-disrupting drug. As expected, all lines achieved nearly complete cell-cycle blocks shortly after nocodazole treatment, with DNA contents of 4C (with 2C representing the DNA content in the G1 phase of the cell cycle, before DNA replication has occurred; representative examples are shown in Fig. 1). Morphological analysis of the 4C blocked cells, however, revealed a striking difference between MIN and CIN cells. All MIN cell lines had a normal checkpoint response, resulting in an accumulation of cells with condensed chromosomes characteristic of a sustained mitotic block. In the CIN lines, there was an abnormal response, with many fewer mitotic cells and no clear peak in mitotic index observed at any time point (Fig. 2a). The response of MIN cells was characteristic of those with intact mitotic checkpoints¹³, and a similar response was observed in normal human fibroblasts (Fig. 2a).

Consistent differences in mitotic indices were also observed in CIN cells versus MIN cells after treatment with colcemid (Figs 1 and 2b), an agent that blocks microtubules through a different mechanism from that of nocodazole. This defect was further established by the higher fraction of CIN cells that synthesized DNA during nocodazole or colcemid treatment (Fig. 2c). There was little overlap between the responses observed in MIN and CIN cells in these

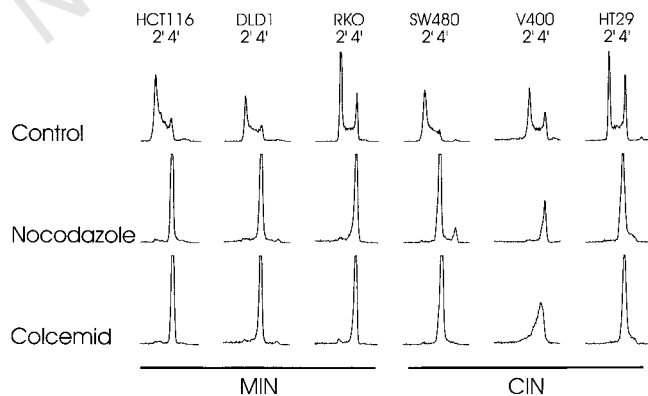


Figure 1 Analysis of the cell cycle of MIN and CIN cells. MIN (HCT116, DLD1, and RKO) and CIN (SW480, V400, and HT29) cells were treated with nocodazole or colcemid for 18 h, stained with Hoechst 33258, a DNA-specific dye, and analysed by flow cytometry. 2' and 4' refer to the DNA contents of each cell line in G1 and G2/M phases, respectively.

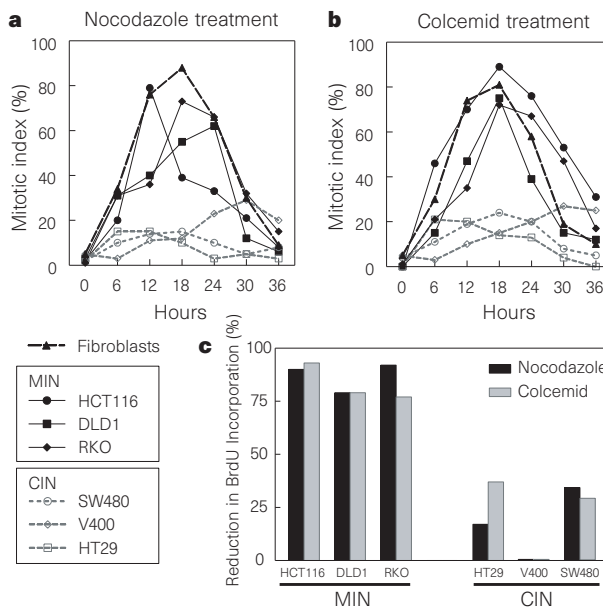


Figure 2 Mitotic indices and DNA synthesis in MIN and CIN cells. Cells were treated with nocodazole (a) or colcemid (b) for the indicated times, stained with H33258, and analysed by fluorescence microscopy. c, BrdU was added to the nocodazole- or colcemid-treated cultures 2.5 h before collection. The bars represent the percentage reduction in BrdU incorporation compared with untreated cells, assessed using an antibody to BrdU. At least 200 cells were counted for each determination and the result shown is representative of those observed in three independent experiments.